Access the most recent version at http://dmm.biologists.org/lookup/doi/10.1242/dmm.020248

A mitochondrial therapeutic reverses diabetic visual decline.

N.M. Alam[1,2]*, W. C. Mills IV[3], A.A. Wong[2], R.M. Douglas[4], H. H. Szeto[3], G. T. Prusky[1,2]

[1]Department of Physiology and Biophysics, Weill Cornell Medical College, New York, NY, USA.

[2]Burke Medical Research Institute, White Plains, NY, USA.

[3]Research Program in Mitochondrial Therapeutics, Department of Pharmacology, Weill Cornell
Medical College, New York, NY, USA.

[4]Department of Ophthalmology and Visual Sciences, University of British Columbia, Vancouver, BC, Canada.

*Corresponding Author
Nazia Alam
Weill Cornell Medical College
Burke Medical Research Institute
785 Mamaroneck Avenue
White Plains, NY 10605
nazia.alam@gmail.com

Key Words: diabetic retinopathy, RPE, SS-31, MTP-131, Bendavia, insulin resistance, hyperglycemia, optomotor, spatial vision, cardiolipin, OKT, mouse

Abstract:

Diabetic retinopathy is characterized by progressive vision loss and the advancement of retinal micoraneurysms, edema, and angiogenesis. Unfortunately, managing glycemia or targeting vascular complications with anti-vascular endothelial growth factor agents has shown only limited efficacy in treating the deterioration of vision in diabetic retinopathy. In light of growing evidence that mitochondrial dysfunction is an independent pathophysiology of diabetes and diabetic retinopathy, we investigated whether selectively targeting and improving mitochondrial dysfunction is a viable treatment for visual decline in diabetes. Measures of spatial visual behavior, blood glucose, bodyweight, and optical clarity were made in mouse models of diabetes. Treatment groups were administered MTP-131, a water-soluble tetrapeptide that selectively targets mitochondrial cardiolipin and promotes efficient electron transfer, either systemically or in eye drops. Progressive visual decline emerged in untreated animals before the overt symptoms of metabolic and ophthalmic abnormalities were manifest, but with time, visual dysfunction was accompanied by compromised glucose clearance, and elevated blood glucose and bodyweight. MTP-131 treatment reversed the visual decline without improving glycemic control or reducing bodyweight. These data provide evidence that visuomotor decline is an early complication of diabetes. They also indicate that selectively treating mitochondrial dysfunction with MTP-131 has the potential to remediate the visual dysfunction, and complement existing treatments for diabetic retinopathy.

Introduction:

Diabetic retinopathy is a leading cause of progressive vision loss and blindness. It is characterized by occlusion and leakage of retinal vessels, which leads to macular edema in its non-proliferative phase, and angiogenesis and retinal detachment in its proliferative phase. Whereas vascular endothelial growth factor expression is necessary for the angiogenesis (Stefanini et al., 2014), treatment with anti- vascular endothelial growth factor agents is able to improve visual function in <30% of patients. Likewise, therapies aimed at managing the symptoms of metabolic dysfunction have shown limited efficacy in slowing the progression of diabetic retinopathy; diabetic complications develop in ~20% of patients under strict glycemic or blood-pressure control (Antonetti et al., 2012). Thus, earlier detection of risk for diabetes and diabetic retinopathy, and intervention with novel therapeutics before irreversible retinal damage occurs, has great potential to improve treatment.

There is growing recognition that retinal dysfunction (Barber et al., 2005; Ly et al., 2011; Martin et al., 2004; Murakami and Yoshimura, 2013; van Dijk et al., 2009) and impaired visual behavior is present in human diabetics and animal models before retinal vascular changes are evident (Akimov and Rentería, 2012; Aung et al., 2013; Hardy et al., 1992; Jackson et al., 2012; Kirwin et al., 2011). Thus, the identification of visual dysfunction early in the course of diabetes may provide an advanced opportunity for therapeutic intervention. A promising candidate for early intervention in diabetic retinopathy is the remediation of mitochondrial dysfunction. Diabetic complications in the non-proliferative phase of diabetic retinopathy are associated with metabolic pathways that are up-regulated by sustained hyperglycemia: increased polyol pathway flux, increased formation of advanced glycation end products and their receptors, activation of protein kinase C, and increased hexosamine pathway flux (Forbes and Cooper, 2013). It has been proposed that the pathways are linked by the mitochondrial production of reactive oxygen species resulting from increased

metabolic flux through the electron transport chain. This is supported by evidence that normalizing mitochondrial superoxide production can mitigate hyperglycemic damage (Brownlee, 2001; Nishikawa et al., 2000).

Indeed, mitochondria are simultaneously a major source of intracellular reactive oxygen species and the target of oxidative damage, and evidence of mitochondrial oxidative stress is present when histopathological abnormalities arise in diabetic retinopathy (Du et al., 2003; Kowluru and Zhong, 2011). Altered mitochondrial structure, including swelling and loss of cristae, the accumulation of defects in mitochondrial DNA, and a reduction of transport proteins (Kowluru and Zhong, 2011; Madsen-Bouterse et al., 2010b; Santos and Kowluru, 2013) which may be independent of hyperglycemia (Zhong and Kowluru, 2011), have also been reported. In addition, impairment of retinal pigment epithelium mitochondria is associated with increased oxidative stress, reduced ATP, and compromised autophagic and phagocytic capacities (He et al., 2010; Kanwar et al., 2007; Li et al., 2014; Madsen-Bouterse et al., 2010a). Taken together, these data indicate that apoptotic stress in the retina has the capacity to induce the hallmark microvascular injury of diabetic retinopathy, and that improving mitochondrial function may be an effective treatment.

Whereas antioxidants have shown promise in preclinical studies as a therapy for diabetic retinopathy (Huang et al., 2013; Nawaz et al., 2013; Xie et al., 2008), they have not been effective in clinical trials; possibly due to their inability to penetrate mitochondria. This problem can be overcome with the use of MTP-131 (also known as SS-31), a water-soluble mitochondria-targeting peptide that attenuates mitochondrial reactive oxygen species production and cytochrome c release (Huang et al., 2013; Li et al., 2011; Szeto and Birk, 2014; Zhao et al., 2004). We thus tested the hypothesis here that MTP-131 can remediate visual impairment in mouse models of diabetes.

Results:

Characterization of Diabetic Mouse Models

Type-1 diabetes is an autoimmune disease that leads to loss of insulin-producing beta cells in the pancreas, which is often modeled in animal studies with injections of streptozotocin (STZ). We administered STZ to C57BL/6 mice fed a normal diet (ND) for 5 days at 8 weeks of age (ND+STZ). Type-2 diabetes is characterized by insulin resistance and the inability of β-cells to up-regulate their insulin production. For modeling this, mice were fed a diabetic diet (DD) high in fat and carbohydrates from 4 weeks of age, and a third group received both DD and STZ (DD+STZ). Control mice were fed a ND throughout the study.

Elevated resting blood glucose (non-fasted) was present in each diabetic model by 15 weeks, which was sustained at 32 weeks (Fig. 1A). Evidence of insulin resistance was also present in the results of a glucose tolerance test administered at 12 (Fig. 1B) and 30 weeks (Fig. 1C), with DD groups showing the greatest impairment. Elevated bodyweight emerged by 15 weeks in groups fed a DD, and by 32 weeks, mice in the DD groups were two-fold heavier than mice fed a ND (Fig. 1D, ~56g vs ~29g).

Progressive Decline of Visual Function in Diabetic Mouse Models

Spatial frequency (SF) and contrast thresholds for optokinetic tracking were measured through each eye once/week from 3-32 weeks, using a virtual optokinetic system (Prusky et al., 2004). SF thresholds near 0.39 cycles/degree (c/d) were measured in ND mice (Fig. 2A) up to 32 weeks; performance comparable to previously-published values (Prusky et al., 2004; Prusky et al., 2006). Loss-of-function emerged by 12 weeks in ND+STZ mice, which by 32 weeks, was reduced by 17%. Visual dysfunction emerged earlier (at 9 weeks) and declined more (29%) in DD mice. In DD+STZ mice, visual dysfunction emerged the earliest (at 8 weeks), and declined the most (38%), by 32 weeks.

We have previously defined the luminance conditions in the virtual optokinetic system that are able isolate cone- and rod-only function (Alam et al., 2015; Altimus et al., 2010), and as such, the lighting conditions used to record the thresholds in Fig. 2A were selective for cone-mediated function. In order to measure rod-mediated function in the same animals, we configured the virtual optokinetic system to record rod-driven thresholds in low light conditions. Fig. 2B is a comparison of cone- and rod-selective function at 28 weeks. Whereas cone function was reduced by 16% in ND+ STZ mice, 27% in DD mice, and 36% in DD +STZ mice, rod function was proportionally less affected; ND+ STZ = 3%; DD = 10%, and DD +STZ = 18%. Thus, the loss of visual function in the diabetic models was primarily due to compromised cone-mediated responses.

Measures of CS also revealed evidence of visual decline that was graded by group. Adult-like CS (Douglas et al., 2005; Prusky et al., 2004) was present in ND mice at 4, 12, and 32 weeks (Fig. 2C). CS in ND+STZ mice (Fig. 2D) was normal at 4 and 12 weeks, but was slightly reduced by 32 weeks at SFs above 0.06 c/d. CS in DD mice was marginally lower at high SFs between 4 and 12 weeks, and by 32 weeks, was reduced at all SFs above 0.03 c/d (Fig. 2E). DD+STZ mice showed loss of function from 4-12 weeks comparable to DD mice, but showed a greater decline by 32 weeks (Fig. 2F).

MTP-131 Treatment Reversed Visual Decline in Diabetic Mouse Models

Treatment groups were injected with MTP-131 (1 mg/kg), (Veh; 0.9% saline), subcutaneously once/day from 12 weeks; an age by which evidence of visuomotor dysfunction had developed in each of the diabetic models (i.e. Fig. 2). The treatment did not alter the level of non-fasted resting blood glucose (Fig. 3A), and did not change the rate of glucose clearance measured at 30 weeks (compared to Veh group; Fig. 3B). Likewise, the treatment did not correct the elevated bodyweight of the DD groups (Fig. 3C). Improvement of visual function, however, was present in each of the diabetic groups. Fig. 4A shows that

improvement of the SF threshold for opto-kinetic tracking was present in DD+STZ mice 1 week after treatment, within 4 weeks in DD mice, and within 6 weeks in ND+STZ mice. Improvement continued thereafter in all groups until thresholds were restored to normal values by 24 weeks in DD+STZ mice, by 25 weeks in ND+STZ mice, and by 31 weeks in DD mice. MTP-131 treatment did not alter function in the control (ND) group. Cone-and rod selective dysfunction in the MTP-131 treated mice were both fully reversed in ND+STZ and DD+STZ groups, and substantially remediated in the DD group (Fig. 4B; compare with 28 weeks in Fig 2B). MTP-131 treatment improved CS in a similar manner; MTP-131 did not affect CS in ND mice (Fig. 4C), but it restored thresholds to near-normal values in ND+STZ (Fig. 4D), in DD (Fig. 4E), and DD+STZ mice (Fig. 4F). Ophthalmic examinations of mice presented in Figs. 3 & 4 revealed only sporadic ocular abnormalities, none of which were related to group or treatment. All animals were assessed at 12 weeks of age, prior to starting any treatment, and at 32 weeks prior to euthanasia, using a modification of the MacDonald-Shadduck Scoring System described elsewhere (Altmann et al., 2010). Ophthalmic examinations identified three animals with abnormal visual thresholds at 12 weeks, in the form of dense corneal infiltrates or central opacities, likely due to grooming or fighting. The mice were removed from the study. Two left eyes and two right eyes showed small punctate corneal opacities (less than 25% corneal involvement (score=1), either in the inferior or nasal region of 4 animals prior to 12 weeks of age, but that animals remained in the study and were randomly assigned into groups. Ophthalmic examinations were performed again at 32 weeks of age, and no animals were identified with ocular problems.

Efficacy of MTP-131 Applied Via Eye Drops

We hypothesized that the benefit of systemic MTP-131 treatment was related to its action on the retina, since MTP-131 did not correct weight gain or high blood glucose. In an effort to deliver MTP-131 to the eye, we investigated whether eye drop application of the peptide

would also treat diabetic visual dysfunction. Fig. 5A, B and C shows that resting blood glucose and body weight measures were unaffected by MTP-131 or placebo (Veh) eye drop application. In Fig. 5C, Veh-treated mice exhibited a SF threshold decline comparable to that with systemic Veh treatment (Fig. 2A, magenta line). However, decline in the MTP-131 eye drop-treated group was reversed after 1 week of treatment, and normal function was reinstated by 20 weeks- 4 weeks earlier than with systemic MTP-131 treatment in the same model.

In a separate cohort of mice, we investigated whether the timing and rate of visual recovery following the application of MTP-131 was dose-dependent (Fig. 5D). Improved function was observed within one week of treatment with 30 mg/ml, and within 5 weeks with 10 mg/ml. 1 mg/ml treatment did not lead to improvement. As with systemic MTP-131 treatment, the restoration of function with eye drop application of MTP-131 was independent of overt changes in the quality of the optical axis (data not shown).

MTP-131 Reversed More Severe Visual Dysfunction

To determine whether MTP-131 application was able to remediate more pronounced visual dysfunction than that at 12 weeks (i.e. Fig. 5), eye drop treatment with MTP-131 (30 mg/ml) was initiated in a group of DD+STZ mice at 34 weeks; an age at which the SF threshold in untreated animals was reduced by ~50% (Fig. 6C). As in previous experiments, MTP-131 treatment had no effect on resting blood glucose (Fig. 6A) or body weight (Fig. 6B). Unlike the effect on visual function with treatment from 12 weeks, which showed a beneficial effect within 1 week (Fig. 5C), visual function continued to decline for 4 weeks after MTP-131 treatment in the group. At 5 weeks, however, visual decline was halted, followed by recovery at a rate similar to that with treatment from 12 weeks, reaching ~75% of normal by 52 weeks (Fig. 6C). As stipulated by our animal protocol, the study was terminated at 52 weeks, and thus, it is not known whether continued treatment would have

led to more improvement. However, the rate of recovery appeared to slow after 48 weeks, likely indicating that complete recovery would not be achieved with more time. Whereas CS was measured in all of the eye drop studies, it changed in concert with measures of SF thresholds, and thus, the data is not presented here.

Discussion:

This study, which unfolded over the course of 2 years and utilized > 150 mice, is the most comprehensive examination to date of visual decline, and restoration with treatment, in rodent models of diabetes. It established a time course of the relationship between the emergence of metabolic dysfunction and visual decline in three diabetic models in the same mouse strain, it illuminated a role for mitochondrial dysfunction in the pathogenesis of diabetic visual complications, and it demonstrated a clinically-feasible approach to treating it.

We used a repeated low-dose STZ protocol to model type-1 diabetes, rather than the typical single high dose STZ protocol, to reduce the off-target toxic effects of STZ (Hayashi et al., 2006; Like and Rossini, 1976). This resulted in only a moderate increase in fed blood glucose (Hayashi et al., 2006; Leiter, 1982) and slightly abnormal glucose clearance, which may better model type-1 diabetes. Feeding a diet high in fat and carbohydrates was used to model type-2 diabetes, which led to an increase in body weight, abnormal glucose clearance, and mild hyperglycemia. Although we did not measure insulin in this study, an increase in plasma insulin has previously been reported in diet-induced models of diabetes (Park et al., 2005; Surwit et al., 1988). For example, a decrease in insulin-stimulated glucose uptake in the heart has been reported within 1.5 weeks of initiating a high fat diet in young C57BL/6 mice, which was reduced by ~90% after 20 weeks (Park et al., 2005). In addition, plasma insulin was elevated within 2 weeks in young mice fed a high fat diet, and remained elevated for up to 52 weeks (Park et al., 2005; Surwit et al., 1988; Winzell and Ahrén, 2004). Thus, the DD model enabled the ability to study the effect of insulin resistance on visual function. Indeed, the elevated blood glucose in DD mice most likely resulted from reduced glucose uptake by skeletal muscles and adipose tissue, due to loss of insulin signaling (Winzell and Ahrén, 2004). A group that combined DD with STZ treatment provided a model of advanced type-2 diabetes, which is characterized by defects in insulin secretion and insulin resistance.

A decline of visuomotor function was detected in each experimental model before changes in resting blood glucose emerged- a common clinical indicator of susceptibility to diabetes. The onset of visual decline was most rapid in the DD+STZ group, and slowest in the ND+STZ group, suggesting that insulin resistance may have an early negative effect on visual function. Insulin receptors are expressed on both vascular and neural cells of the retina (Haskell et al., 1984), and are able to autophosphorylate and activate downstream kinases, as in other insulin-sensitive tissues (Reiter et al., 2003). Rats administered STZ have shown reduced insulin receptor signaling in the retina, especially in retinal endothelial cells, which may contribute to the early progression of diabetic retinopathy (Aizu et al., 2002; Fort et al., 2011; Kondo and Kahn, 2004; Reiter et al., 2003).

The study was designed such that daily MTP-131 treatment began 4 weeks after STZ treatment, or 8 weeks after the initiation of a DD. Since visual decline only began 4 weeks after STZ, MTP-131 treatment appeared to both reverse further decline, and prevent sustained visual dysfunction. MTP-131 treatment was also able to reverse more pronounced visual dysfunction in the DD group, but the time to full recovery was shortened. Unexpectedly, even though the DD+STZ mice had the most dramatic rate of visual decline; they had the most rapid response to MTP-131 treatment, showing improvement within one week of MTP-131 administration and full recovery after 12 weeks. The lack of effect of MTP-131 on blood glucose and body weight is in keeping with previous reports in STZ-administered rats (Huang et al., 2013). The more rapid onset of visual decline, and the slower treatment response in the DD group is also consistent with insulin resistance as a cause of diabetic visual dysfunction. Since the addition of STZ has been shown to reduce diet-induced insulin resistance in C57BL/6 mice (Ning et al., 2011), this may account for the more rapid MTP-131 treatment effect in the DD+STZ group.

MTP-131 is a mitochondria-targeting peptide known to protect the structure of cristae and prevent mitochondrial swelling under ischemic conditions in numerous cell types (Birk et al., 2013; Liu et al., 2014; Szeto et al., 2011). By maintaining cristae membranes, MTP-131 treated tissues may be better able to sustain ATP synthesis and preserve vital ATP-dependent processes (Birk et al., 2013; Szeto et al., 2011). Although MTP-131 was known at the outset to selectively partition to the inner mitochondria membrane (Zhao et al., 2005), the mechanism by which MTP-131 protects mitochondrial cristae remained unclear until recently. It is now known, however, that MTP-131 has a high affinity for cardiolipin, a unique anionic phospholipid (Birk et al., 2013; Szeto, 2014). The conical shape of cardiolipin is required to maintain the curvature of cristae, and cardiolipin deficiency results in a loss of cristae and reduced mitochondrial respiration (Schlame and Ren, 2006). Since cardiolipin contains four unsaturated acyl chains, it is readily peroxidized under oxidative conditions, which is consistent with reports that increased cardiolipin peroxidation and cardiolipin depletion is present in diabetic hearts (Ferreira et al., 2013; He and Han, 2014). High glucose has also been postulated to increase mitochondrial reactive oxygen species (Brownlee, 2001), and thus, cardiolipin peroxidation could have the effect of reducing mitochondrial respiration. Interestingly, retinal mitochondria from diabetic mice show elevated superoxide levels and reduced glutathione, indicative of mitochondrial oxidative stress (Kanwar et al., 2007). In addition to a high reactive oxygen species environment, cardiolipin peroxidation is catalyzed by cytochrome c that is tightly bound to cardiolipin, and this [cyt c/cardiolipin] complex converts cytochrome c from an electron carrier to a peroxidase that can peroxidize cardiolipin (Kagan et al., 2005; Sinibaldi et al., 2010; Snider et al., 2013). MTP-131 appears to protect the architecture of mitochondrial cristae by reducing mitochondrial oxidative stress and preventing cytochrome c peroxidase activity (Birk et al., 2013; Zhao et al., 2004).

Mitochondrial abnormalities have been documented in insulin-resistant and diabetic states in human and animal studies, and it has been proposed that mitochondrial dysfunction may be the primary defect in obesity-related insulin resistance (Patti and Corvera, 2010). The causal mechanism underlying the mitochondrial dysfunction, however, is not fully understood. Although it is often assumed that hyperglycemia causes mitochondrial oxidative stress in diabetes, a recent study reported lower mitochondrial superoxide and mitochondrial respiratory activity in the kidneys of diabetic mice after STZ treatment (Dugan et al., 2013), and suggests a loss of functional mitochondria in the latter stages of diabetes (Sharma, 2015) . MTP-131 could thus provide a novel approach for treating diabetes, based not on mitigating elevated blood glucose, but on enhancing mitochondrial bioenergetics through the preservation of mitochondrial cristae, and improved efficiency of the electron transfer chain. MTP-131 has displayed an exceptional safety profile in Phase 1 clinical trials, likely due to its lack of effect on the function of normal mitochondria (Siegel et al., 2013). Since the beneficial effects of MTP-131 appear to be independent of reducing circulating glucose, the treatment may also be useful in complementing therapies aimed at managing the typical symptoms of diabetes. Indeed, based on the results reported here, a clinical formulation of topical ophthalmic MTP-131 (Ocuvia^{TM}) has entered a clinical trial for treating diabetic macular edema.

Materials and methods:

Animal Subjects

Experimental procedures on animals were conducted in accordance with the policies of the Weill Cornell Medical College Institutional Animal Care and Use Committee. 151 male C57BL/6 mice obtained from Charles River Laboratories at 3 weeks of age were group-housed at the Burke Medical Research Institute vivarium. They were maintained at 68º-76ºF with 30-70% relative humidity, and a photoperiod of 12 hour light (6:00 lights on)/12 hour dark (18:00 lights off).

Disease Modeling

Mice in control groups were fed a ND (LabDiet Picolab Rodent Diet 5053 (min. protein = 20%, crude fat = 4.5%, max. crude fiber = 6.0%) *ad libitum* over the course of the study. Type 1 diabetes is an autoimmune disease that destroys insulin-producing pancreatic beta cells, which we modeled by administering the beta cell toxin STZ (Sigma S0130) to mice at 8 weeks of age fed a ND (ND+STZ; Arora et al., 2009; Gilbert et al., 2011). STZ was prepared in a 7.5 mg/ml sodium citrate buffer (pH 4.5) immediately prior to injection. On 5 consecutive days, mice were fasted 4 hours, anesthetized with inhaled isoflurane (induction at 2.5–4.5%, maintenance at 1–2% evaporated in 1-1.5 L/min O_2), before being administered 40 mg/kg intraperitoneal STZ.

Type-2 diabetes is characterized by insulin resistance and the inability of beta cells to up-regulate their function. To model this, mice were fed a DD (Bio-Serv Mouse Diet F3282; protein = 20.5%, crude fat = 36%, fiber = 0%, carbohydrates = 35.7%) *ad libitum* from 4 weeks of age. To model an accelerated version of type-2 diabetes, another group was fed a DD from 4 weeks and administered STZ at 8 weeks of age (DD+STZ).

MTP-131 Administration

In one experiment, mice were injected daily with a 1mg/kg solution of MTP-131 sub-cutaneously (provided by Stealth Peptides Inc, Newton, MA) dissolved in 0.9% sterile saline (pH 5.5-6.5), or with saline alone. In another experiment, mice were administered MTP-131 as an ophthalmic-formulated solution (Ocuvia^{TM}, provided by Stealth Peptides, Inc) daily via eye drops (in 0.01M sodium acetate buffer solution (pH 6.00); 5 ul/eye), or with buffer alone.

Measures of Weight and Blood Glucose

Mice were weighed, then lightly anesthetized with inhaled isoflurane, and a drop of blood was harvested from the tail or submandibular vein. Glucose in the drop was measured with a glucometer (AlphaTRAK II Blood Glucose Monitoring System, or One Touch Ultra Mini Blood Glucose Monitoring System). A glucose tolerance test was also administered periodically; animals were fasted overnight prior to receiving D-glucose (1.5 g/kg i.p.). Blood glucose was measured as above prior to and after 10, 20, 30, 60, and 120 minutes glucose administration.

Tests of Spatial Visual Function

Spatial thresholds for opto-kinetic tracking of sine-wave gratings were measured weekly using a virtual optokinetic system (OptoMotry, CerebralMechanics Inc., Medicine Hat, Alberta, Canada; (Prusky et al., 2004). Vertical sine wave gratings moving at 12 degrees/second, or gray of the same mean luminance, were projected on 4 monitors as a virtual cylinder, which surrounded an unrestrained mouse standing on a platform at the epicenter. The hub of the cylinder was continually centered between the eyes of the mouse to set the SF of the grating at the mouse's viewing position as it shifted its position. Gray was projected while the mouse was moving, but when movement ceased, the gray was replaced with a grating. Grating rotation under these circumstances elicited reflexive tracking, which was scored via live video using a method of limits procedure with a yes/no criterion. A SF

threshold, and contrast thresholds at 6 spatial frequencies (0.031, 0.064, 0.092, 0.103, 0.192, 0.272 c/d), were generated through each eye separately in a testing session (14 thresholds in ~ 30 minutes). Michelson contrast sensitivity (CS) was calculated using the average screen luminance (maximum –minimum)/(maximum + minimum). Most thresholds were generated under photopic lighting conditions (screen luminance= 54 lux), which selectively measures cone-based visual function. Rod-based visual function under scotopic conditions (1 lux) was also assessed in some animals after dark adaptation (>6 hours; Alam et al., 2015). For this, 6.3 ND filters (Lee Filters, USA) were placed on the monitors, and infrared lighting and an infrared-sensitive camera (Sony Handycam DCR-HC28, Sony, Japan) were used to image the animal.

Ophthalmic Assessments

A biomicroscope (slit lamp) was used to examine the cornea for clarity, size, surface texture, and vascularization, and the iris was inspected for pupil size, constriction, reflected luminescence, and synechia. The pupil was then dilated with a drop of 0.05% Tropicamide ophthalmic solution, and the lens was scored for cataract using a modified version of the Merriam-Focht scoring criterion (MERRIAM and FOCHT, 1962; Worgul et al., 1993). An indirect ophthalmoscope was also used to inspect the fundus for damage, degeneration, retinal vessel constriction, and optic nerve head abnormalities. A modified MacDonald-Shaddock Scoring System was used to score the optical quality of eyes at 12 and 32 weeks of age.

Statistical Analyses

Using Graphpad Prism 6 software, two-way, repeated-measures ANOVAs were used to make group comparisons. Post-hoc multiple comparisons were performed using the Tukey's or Bonferroni correction methods. Statistical comparisons were considered significantly different at $p < 0.05$.

Acknowledgements:

Funding: The research was supported by the Burke Foundation, Stealth Peptides Inc., and the Research Program in Mitochondrial Therapeutics at Weill Cornell Medical College. We thank the Stealth Peptides team for their expertise and valuable discussions, and Dr. Sunghee Cho for her assistance on the project. **Author contributions:** NMA, WCM and AAW designed and executed experiments, analyzed data and wrote manuscript. RMD participated in designing and executing experiments and editing the manuscript. GTP and HHS designed experiments and wrote and edited the manuscript. **Competing Interests:** The peptide described in this article has been licensed for commercial research and development to Stealth Peptides Inc, a clinical stage biopharmaceutical company, in which H.H.S. and the Cornell Research Foundation have financial interests. The Research Program in Mitochondrial Therapeutics at Weill Cornell Medical College was established with a gift from Stealth Peptides International, Inc. Equipment and software in this article were purchased from CerebralMechanics Inc., of which GTP and RMD are Principals.

References:

Aizu, Y., Oyanagi, K., Hu, J. and Nakagawa, H. (2002). Degeneration of retinal neuronal processes and pigment epithelium in the early stage of the streptozotocin-diabetic rats. *Neuropathology* **22**, 161–70.

Akimov, N. P. and Rentería, R. C. (2012). Spatial frequency threshold and contrast sensitivity of an optomotor behavior are impaired in the Ins2Akita mouse model of diabetes. *Behav. Brain Res.* **226**, 601–5.

Alam, N. M., Altimus, C. M., Douglas, R. M., Hattar, S. and Prusky, G. T. (2015). Photoreceptor regulation of spatial visual behavior. *Invest Ophthalmol Vis Sci* in press.

Altimus, C. M., Güler, A. D., Alam, N. M., Arman, A. C., Prusky, G. T., Sampath, A. P. and Hattar, S. (2010). Rod photoreceptors drive circadian photoentrainment across a wide range of light intensities. *Nat. Neurosci.* **13**, 1107–12.

Altmann, S., Emanuel, A., Toomey, M., McIntyre, K., Covert, J., Dubielzig, R. R., Leatherberry, G., Murphy, C. J., Kodihalli, S. and Brandt, C. R. (2010). A Quantitative Rabbit Model of Vaccinia Keratitis. *Invest. Ophthalmol. Vis. Sci.* **51**, 4531–4540.

Antonetti, D. A., Klein, R. and Gardner, T. W. (2012). Diabetic retinopathy. *N. Engl. J. Med.* **366**, 1227–39.

Arora, S., Ojha, S. K. and Vohora, D. (2009). Characterisation of Streptozotocin Induced Diabetes Mellitus in Swiss Albino Mice. **3**, 81–84.

Aung, M. H., Kim, M. K., Olson, D. E., Thule, P. M. and Pardue, M. T. (2013). Early visual deficits in streptozotocin-induced diabetic long evans rats. *Invest. Ophthalmol. Vis. Sci.* **54**, 1370–7.

Barber, A. J., Antonetti, D. A., Kern, T. S., Reiter, C. E. N., Soans, R. S., Krady, J. K., Levison, S. W., Gardner, T. W. and Bronson, S. K. (2005). The Ins2Akita mouse as a model of early retinal complications in diabetes. *Invest. Ophthalmol. Vis. Sci.* **46**, 2210–8.

Birk, A. V, Liu, S., Soong, Y., Mills, W., Singh, P., Warren, J. D., Seshan, S. V, Pardee, J. D. and Szeto, H. H. (2013). The mitochondrial-targeted compound SS-31 re-energizes ischemic mitochondria by interacting with cardiolipin. *J. Am. Soc. Nephrol.* **24**, 1250–61.

Brownlee, M. (2001). Biochemistry and molecular cell biology of diabetic complications. *Nature* **414**, 813–20.

Douglas, R. M., Alam, N. M., Silver, B. D., McGill, T. J., Tschetter, W. W. and Prusky, G. T. (2005). Independent visual threshold measurements in the two eyes of freely moving rats and mice using a virtual-reality optokinetic system. *Vis. Neurosci.* **22**, 677–84.

Du, Y., Miller, C. M. and Kern, T. S. (2003). Hyperglycemia increases mitochondrial superoxide in retina and retinal cells. *Free Radic. Biol. Med.* **35**, 1491–9.

Dugan, L. L., You, Y.-H., Ali, S. S., Diamond-Stanic, M., Miyamoto, S., DeCleves, A.-E., Andreyev, A., Quach, T., Ly, S., Shekhtman, G., et al. (2013). AMPK dysregulation promotes diabetes-related reduction of superoxide and mitochondrial function. *J. Clin. Invest.* **123**, 4888–99.

Ferreira, R., Guerra, G., Padrão, A. I., Melo, T., Vitorino, R., Duarte, J. A., Remião, F., Domingues, P., Amado, F. and Domingues, M. R. (2013). Lipidomic characterization of streptozotocin-induced heart mitochondrial dysfunction. *Mitochondrion* **13**, 762–71.

Forbes, J. M. and Cooper, M. E. (2013). Mechanisms of diabetic complications. *Physiol. Rev.* **93**, 137–88.

Fort, P. E., Losiewicz, M. K., Reiter, C. E. N., Singh, R. S. J., Nakamura, M., Abcouwer, S. F., Barber, A. J. and Gardner, T. W. (2011). Differential roles of hyperglycemia and hypoinsulinemia in diabetes induced retinal cell death: evidence for retinal insulin resistance. *PLoS One* **6**, e26498.

Gilbert, E. R., Fu, Z. and Liu, D. (2011). Development of a nongenetic mouse model of type 2 diabetes. *Exp. Diabetes Res.* **2011**, 416254.

Hardy, K. J., Lipton, J., Scase, M. O., Foster, D. H. and Scarpello, J. H. (1992). Detection of colour vision abnormalities in uncomplicated type 1 diabetic patients with angiographically normal retinas. *Br. J. Ophthalmol.* **76**, 461–4.

Haskell, J. F., Meezan, E. and Pillion, D. J. (1984). Identification and characterization of the insulin receptor of bovine retinal microvessels. *Endocrinology* **115**, 698–704.

Hayashi, K., Kojima, R. and Ito, M. (2006). Strain differences in the diabetogenic activity of streptozotocin in mice. *Biol. Pharm. Bull.* **29**, 1110–9.

He, Q. and Han, X. (2014). Cardiolipin remodeling in diabetic heart. *Chem. Phys. Lipids* **179**, 75–81.

He, Y., Ge, J., Burke, J. M., Myers, R. L., Dong, Z. Z. and Tombran-Tink, J. (2010). Mitochondria impairment correlates with increased sensitivity of aging RPE cells to oxidative stress. *J. Ocul. Biol. Dis. Infor.* **3**, 92–108.

Huang, J., Li, X., Li, M., Li, J., Xiao, W., Ma, W., Chen, X., Liang, X., Tang, S. and Luo, Y. (2013). Mitochondria-targeted antioxidant peptide SS31 protects the retinas of diabetic rats. *Curr. Mol. Med.* **13**, 935–45.

Jackson, G. R., Scott, I. U., Quillen, D. A., Walter, L. E. and Gardner, T. W. (2012). Inner retinal visual dysfunction is a sensitive marker of non-proliferative diabetic retinopathy. *Br. J. Ophthalmol.* **96**, 699–703.

Kagan, V. E., Tyurin, V. A., Jiang, J., Tyurina, Y. Y., Ritov, V. B., Amoscato, A. A., Osipov, A. N., Belikova, N. A., Kapralov, A. A., Kini, V., et al. (2005). Cytochrome c acts as a cardiolipin oxygenase required for release of proapoptotic factors. *Nat. Chem. Biol.* **1**, 223–32.

Kanwar, M., Chan, P.-S., Kern, T. S. and Kowluru, R. A. (2007). Oxidative damage in the retinal mitochondria of diabetic mice: possible protection by superoxide dismutase. *Invest. Ophthalmol. Vis. Sci.* **48**, 3805–11.

Kirwin, S. J., Kanaly, S. T., Hansen, C. R., Cairns, B. J., Ren, M. and Edelman, J. L. (2011). Retinal gene expression and visually evoked behavior in diabetic long evans rats. *Invest. Ophthalmol. Vis. Sci.* **52**, 7654–63.

Kondo, T. and Kahn, C. R. (2004). Altered insulin signaling in retinal tissue in diabetic states. *J. Biol. Chem.* **279**, 37997–8006.

Kowluru, R. A. and Zhong, Q. (2011). Beyond AREDS: is there a place for antioxidant therapy in the prevention/treatment of eye disease? *Invest. Ophthalmol. Vis. Sci.* **52**, 8665–71.

Leiter, E. H. (1982). Multiple low-dose streptozotocin-induced hyperglycemia and insulitis in C57BL mice: influence of inbred background, sex, and thymus. *Proc. Natl. Acad. Sci. U. S. A.* **79**, 630–4.

Li, J., Chen, X., Xiao, W., Ma, W., Li, T., Huang, J., Liu, X., Liang, X., Tang, S. and Luo, Y. (2011). Mitochondria-targeted antioxidant peptide SS31 attenuates high glucose-induced injury on human retinal endothelial cells. *Biochem. Biophys. Res. Commun.* **404**, 349–56.

Li, X., Zhang, M. and Zhou, H. (2014). The morphological features and mitochondrial oxidative stress mechanism of the retinal neurons apoptosis in early diabetic rats. *J. Diabetes Res.* **2014**, 678123.

Like, A. A. and Rossini, A. A. (1976). Streptozotocin-induced pancreatic insulitis: new model of diabetes mellitus. *Science* **193**, 415–7.

Liu, S., Soong, Y., Seshan, S. V and Szeto, H. H. (2014). Novel cardiolipin therapeutic protects endothelial mitochondria during renal ischemia and mitigates microvascular rarefaction, inflammation, and fibrosis. *Am. J. Physiol. Renal Physiol.* **306**, F970–80.

Ly, A., Yee, P., Vessey, K. A., Phipps, J. A., Jobling, A. I. and Fletcher, E. L. (2011). Early inner retinal astrocyte dysfunction during diabetes and development of hypoxia, retinal stress, and neuronal functional loss. *Invest. Ophthalmol. Vis. Sci.* **52**, 9316–26.

Madsen-Bouterse, S. A., Zhong, Q., Mohammad, G., Ho, Y.-S. and Kowluru, R. A. (2010a). Oxidative damage of mitochondrial DNA in diabetes and its protection by manganese superoxide dismutase. *Free Radic. Res.* **44**, 313–21.

Madsen-Bouterse, S. A., Mohammad, G., Kanwar, M. and Kowluru, R. A. (2010b). Role of mitochondrial DNA damage in the development of diabetic retinopathy, and the metabolic memory phenomenon associated with its progression. *Antioxid. Redox Signal.* **13**, 797–805.

Martin, P. M., Roon, P., Van Ells, T. K., Ganapathy, V. and Smith, S. B. (2004). Death of retinal neurons in streptozotocin-induced diabetic mice. *Invest. Ophthalmol. Vis. Sci.* **45**, 3330–6.

MERRIAM, G. R. and FOCHT, E. F. (1962). A clinical and experimental study of the effect of single and divided doses of radiation on cataract production. *Trans. Am. Ophthalmol. Soc.* **60**, 35–52.

Murakami, T. and Yoshimura, N. (2013). Structural changes in individual retinal layers in diabetic macular edema. *J. Diabetes Res.* **2013**, 920713.

Nawaz, M. I., Abouammoh, M., Khan, H. A., Alhomida, A. S., Alfaran, M. F. and Ola, M. S. (2013). Novel drugs and their targets in the potential treatment of diabetic retinopathy. *Med. Sci. Monit.* **19**, 300–8.

Ning, Y., Zhen, W., Fu, Z., Jiang, J., Liu, D., Belardinelli, L. and Dhalla, A. K. (2011). Ranolazine increases β-cell survival and improves glucose homeostasis in low-dose streptozotocin-induced diabetes in mice. *J. Pharmacol. Exp. Ther.* **337**, 50–8.

Nishikawa, T., Edelstein, D., Du, X. L., Yamagishi, S., Matsumura, T., Kaneda, Y., Yorek, M. A., Beebe, D., Oates, P. J., Hammes, H. P., et al. (2000). Normalizing mitochondrial superoxide production blocks three pathways of hyperglycaemic damage. *Nature* **404**, 787–90.

Park, S.-Y., Cho, Y.-R., Kim, H.-J., Higashimori, T., Danton, C., Lee, M.-K., Dey, A., Rothermel, B., Kim, Y.-B., Kalinowski, A., et al. (2005). Unraveling the temporal

pattern of diet-induced insulin resistance in individual organs and cardiac dysfunction in C57BL/6 mice. *Diabetes* **54**, 3530–40.

Patti, M.-E. and Corvera, S. (2010). The role of mitochondria in the pathogenesis of type 2 diabetes. *Endocr. Rev.* **31**, 364–95.

Prusky, G. T., Alam, N. M., Beekman, S. and Douglas, R. M. (2004). Rapid quantification of adult and developing mouse spatial vision using a virtual optomotor system. *Invest Ophthalmol Vis Sci* **45**, 4611–4616.

Prusky, G. T., Alam, N. M. and Douglas, R. M. (2006). Enhancement of vision by monocular deprivation in adult mice. *J. Neurosci.* **26**, 11554–61.

Reiter, C. E. N., Sandirasegarane, L., Wolpert, E. B., Klinger, M., Simpson, I. A., Barber, A. J., Antonetti, D. A., Kester, M. and Gardner, T. W. (2003). Characterization of insulin signaling in rat retina in vivo and ex vivo. *Am. J. Physiol. Endocrinol. Metab.* **285**, E763–74.

Santos, J. M. and Kowluru, R. A. (2013). Impaired transport of mitochondrial transcription factor A (TFAM) and the metabolic memory phenomenon associated with the progression of diabetic retinopathy. *Diabetes. Metab. Res. Rev.* **29**, 204–13.

Schlame, M. and Ren, M. (2006). Barth syndrome, a human disorder of cardiolipin metabolism. *FEBS Lett.* **580**, 5450–5.

Sharma, K. (2015). Mitochondrial hormesis and diabetic complications. *Diabetes* **64**, 663–72.

Siegel, M. P., Kruse, S. E., Percival, J. M., Goh, J., White, C. C., Hopkins, H. C., Kavanagh, T. J., Szeto, H. H., Rabinovitch, P. S. and Marcinek, D. J. (2013). Mitochondrial-targeted peptide rapidly improves mitochondrial energetics and skeletal muscle performance in aged mice. *Aging Cell* **12**, 763–71.

Sinibaldi, F., Howes, B. D., Piro, M. C., Polticelli, F., Bombelli, C., Ferri, T., Coletta, M., Smulevich, G. and Santucci, R. (2010). Extended cardiolipin anchorage to cytochrome c: a model for protein-mitochondrial membrane binding. *J. Biol. Inorg. Chem.* **15**, 689–700.

Snider, E. J., Muenzner, J., Toffey, J. R., Hong, Y. and Pletneva, E. V (2013). Multifaceted effects of ATP on cardiolipin-bound cytochrome c. *Biochemistry* **52**, 993–5.

Stefanini, F. R., Badaró, E., Falabella, P., Koss, M., Farah, M. E. and Maia, M. (2014). Anti-VEGF for the management of diabetic macular edema. *J. Immunol. Res.* **2014**, 632307.

Surwit, R. S., Kuhn, C. M., Cochrane, C., McCubbin, J. A. and Feinglos, M. N. (1988). Diet-induced type II diabetes in C57BL/6J mice. *Diabetes* **37**, 1163–7.

Szeto, H. H. (2014). First-in-class cardiolipin-protective compound as a therapeutic agent to restore mitochondrial bioenergetics. *Br. J. Pharmacol.* **171**, 2029–50.

Szeto, H. H. and Birk, A. V (2014). Serendipity and the discovery of novel compounds that restore mitochondrial plasticity. *Clin. Pharmacol. Ther.* **96**, 672–83.

Szeto, H. H., Liu, S., Soong, Y., Wu, D., Darrah, S. F., Cheng, F.-Y., Zhao, Z., Ganger, M., Tow, C. Y. and Seshan, S. V (2011). Mitochondria-targeted peptide accelerates ATP recovery and reduces ischemic kidney injury. *J. Am. Soc. Nephrol.* **22**, 1041–52.

Van Dijk, H. W., Kok, P. H. B., Garvin, M., Sonka, M., Devries, J. H., Michels, R. P. J., van Velthoven, M. E. J., Schlingemann, R. O., Verbraak, F. D. and Abràmoff, M. D. (2009). Selective loss of inner retinal layer thickness in type 1 diabetic patients with minimal diabetic retinopathy. *Invest. Ophthalmol. Vis. Sci.* **50**, 3404–9.

Winzell, M. S. and Ahrén, B. (2004). The high-fat diet-fed mouse: a model for studying mechanisms and treatment of impaired glucose tolerance and type 2 diabetes. *Diabetes* **53 Suppl 3**, S215–9.

Worgul, B. V, Brenner, D. J., Medvedovsky, C., Merriam, G. R. and Huang, Y. (1993). Accelerated heavy particles and the lens. VII: The cataractogenic potential of 450 MeV/amu iron ions. *Invest. Ophthalmol. Vis. Sci.* **34**, 184–93.

Xie, L., Zhu, X., Hu, Y., Li, T., Gao, Y., Shi, Y. and Tang, S. (2008). Mitochondrial DNA oxidative damage triggering mitochondrial dysfunction and apoptosis in high glucose-induced HRECs. *Invest. Ophthalmol. Vis. Sci.* **49**, 4203–9.

Zhao, K., Zhao, G.-M., Wu, D., Soong, Y., Birk, A. V, Schiller, P. W. and Szeto, H. H. (2004). Cell-permeable peptide antioxidants targeted to inner mitochondrial membrane inhibit mitochondrial swelling, oxidative cell death, and reperfusion injury. *J. Biol. Chem.* **279**, 34682–90.

Zhao, K., Luo, G., Giannelli, S. and Szeto, H. H. (2005). Mitochondria-targeted peptide prevents mitochondrial depolarization and apoptosis induced by tert-butyl hydroperoxide in neuronal cell lines. *Biochem. Pharmacol.* **70**, 1796–806.

Zhong, Q. and Kowluru, R. A. (2011). Diabetic retinopathy and damage to mitochondrial structure and transport machinery. *Invest. Ophthalmol. Vis. Sci.* **52**, 8739–46.

Figure legends:

Figure 1. Metabolic dysfunction in mouse models of diabetes. A. Elevated blood glucose emerged in ND+STZ, DD and DD+STZ groups by 15 weeks of age (DD = 215 mg/dL +/- 4.35 (n=7); DD+STZ = 235 mg/dL +/- 2.28 (n=6); ND+STZ = 205 mg/dL +/- 3.14; (n=12), significantly higher than ND = 161 mg/dL +/- 1.73 (n=7), $p<0.01$) and was sustained out to 32 weeks (DD = 263 mg/dL +/- 1.35 (n=4); DD+STZ = 253 mg/dL +/- 2.22 (n=3); ND+STZ = 208 mg/dL +/- 3.64 (n=9), significantly higher than ND = 164 mg/dL +/- 2.73 (n=5), $p<0.01$). B; C. Evidence of impaired glucose clearance on a glucose tolerance test was present in each diabetic model when measured at 12 (B; GTT1) and 30 weeks (C; GTT2), with DD groups being the most impaired. Dashed lines demarcate the upper limit of glucometer sensitivity. D. Abnormal weight gain emerged in the diabetic models by 15 weeks (DD = 35.2g +/- 3.11, DD+STZ = 41.3g +/- 1.42, ND+STZ = 24.9g +/- 2.31), which was significantly different than ND = 29.0g +/- 2.14, $p<0.05$. +/- SEMs are plotted in these and other panels but are often occluded by the data symbols.

Figure 2. Progressive decline of visuomotor function in diabetic models. A. SF thresholds under photopic (cone-mediated) conditions did not change in ND mice from 12 (0.393 c/d +/- 0.006, (n=7)) to 32 weeks (0.394 c/d +/- 0.001 (n=5), $p>0.05$). Reduced thresholds (average of both eyes) emerged in ND+STZ mice at 12 weeks (0.387 c/d +/- 0.003 (n=12), $p<0.05$), with 17% decline by 32 weeks (0.325 c/d +/- 0.001 (n=9), $p<0.01$). Reduced thresholds emerged in DD mice by 9 weeks (0.386 c/d +/- 0.002 (n=7), $p<0.01$), with 29% decline by 32 weeks (0.280 c/d +/- 0.001 (n=4), $p<0.01$), and emerged in DD+STZ mice at 8 weeks (0.327 c/d +/- 0.001 (n=6), $p<0.01$), with 38% decline by 32 weeks (0.244 c/d +/- 0.001c/d (n=3), $p<0.01$). B. Cone-mediated function was more compromised than rod function in diabetic models at 28 weeks. As previously reported (Altimus et al., 2010), rod thresholds (Photopic;

R) are significantly lower (0.19225 c/d +/- 0.000324) than cone (C) thresholds (0.3935c/d +/- 0.0006, $p<0.01$, n=4) in ND mice. Both rod and cone thresholds were reduced from normal in all diabetic models, with the most impairment in cone-mediated function: ND+STZ (cone: 0.331c/d +/- 0.0005 vs rod: 0.18624c/d +/- 0.0000342, $p<0.01$); DD (cone: 0.286c/d +/- 0.00634 vs rod: 0.17268c/d +/- 0.000325, $p<0.01$); DD+STZ (cone: 0.253c/d +/- 0.0000233 vs rod: 0.15813c/d +/- 0.000435, $p<0.01$). C; D; E; F) Progressive decline of CS in diabetic models. C. Normal CS was present in ND mice when measured at 4, 12 and 32 weeks. D. CS in ND+STZ mice decreased moderately between 12 and 32 weeks at SFs above 0.06 c/d. E. Decreased CS was evident at 12 weeks in DD mice and progressed by 32 weeks, particularly at the highest SF tested. F. DD+STZ mice displayed the most dysfunction over time, such that by 32 weeks, they did not respond at the highest SF tested.

Figure 3. Metabolic dysfunction was not improved by daily systemic treatment with MTP-131. Daily MTP-131 treatment is indicated by shading. Dotted lines are traces from Fig. 1, depicting the effect of Veh treatment. A. MTP-131 treatment did not reduce resting fed blood glucose in any of the experimental groups. B. MTP-131 had no effect on glucose clearance at 32 weeks in any experimental group. C. MTP-131 did not mitigate weight gain in the groups fed a DD.

Figure 4. Reversal of visual dysfunction following daily systemic treatment with MTP-131. Daily MTP-131 treatment is indicated by shading. Dotted lines are traces from Fig. 1, depicting the effects of Veh treatment. A. Improvement of SF function was present within 2 weeks of treatment in ND+STZ mice (MTP-131 vs Veh; 0.382 c/d +/- 0.001 (n=7) vs 0.377 c/d +/- 0.006 (n=12)), within 3 weeks in DD mice (MTP-131 vs Veh: 0.342 c/d +/- 0.001 (n=8) vs. 0.347c/d +/- 0.003 (n=7)), and within 1 week in DD+STZ mice (MTP-131 vs Veh:

0.340 c/d +/- 0.001 (n=11) vs 0.313c/d +/- 0.002 (n=6)). Full restoration of function was achieved by 24 weeks in ND+STZ (n=4) and DD+STZ (n=8) mice, and by 31 weeks in DD mice (n=5). ND (MTP-131) did not differ statistically from ND (Veh) at any age (n=6, $p>0.05$). B. Cone- and rod-mediated function was restored by MTP-131 treatment, as measured at 28 weeks of age ($p>0.05$); dotted lines depict the results of Veh-treatment abstracted from Fig. 1. C; D; E; F. MTP-131 restored normal CS in each experimental group by 32 weeks.

Figure 5. Daily administration of MTP-131 in eye drops from 12 weeks reversed visual decline. A; B. 30 mg/ml MTP-131 did not affect resting blood glucose (A; MTP-131 vs Veh, $p>0.05$ vs a $p<0.01$ for two way ANOVA on age, interaction and treatment condition with ND group after 12 weeks) or body weight (B; (A; MTP-131 vs Veh, $p>0.05$ vs a $p<0.001$ for two way ANOVA on age, interaction and treatment condition with ND group). Dotted lines represent control data from ND mice in Fig. 1. C. SF function was restored to control values by 20 weeks, 4 weeks earlier than with systemic treatment ($p>0.05$ Eye Drops (Veh) vs Systemic (Veh); $p<0.001$ for Eye Drops (MTP-131) vs ND from 7-19 weeks of age, $p<0.05$ from 20 weeks of age; Eye Drops (MTP-131) vs Systemic (MTP-131) $p<0.01$ between 17 and 23 weeks of age (Fig. 2A)). D. Dose-dependent effect of MTP-131 eye drop treatment; 1 mg/ml had no effect ($p<0.01$ for 30mg/ml group from 13 weeks of age compared to Veh and 1mg/ml groups; $p<0.01$ for 10mg/ml group from 16 weeks of age compared to Veh and 1mg/ml groups; $p<0.001$ for 30mg/ml group vs 10mg/ml group from 13 to 29 weeks; $p>0.05$ 1mg/ml vs Veh at all points).

Figure 6. Daily administration of MTP-131 in eye drops reversed more severe visual dysfunction present later in the course of disease. A, B) Treatment with MTP-131 in eye

drops (30 mg/ml) from 34 weeks (shading) in DD+STZ mice did not change markers of metabolic dysfunction (A. Resting blood glucose @52 weeks- MTP-131: 260 mg/dL +/- 2.64 (n=8) vs Veh: 254 mg/dL +/- 2.11 (n=7), p=0.1363 vs ND: 173 mg/dL +/- 3.06 (n=4)) or body weight (B. @52 weeks- MTP-131: 56.1g +/- 2.5 vs Veh: 56.0g +/- 2.3, p=0.1021 vs ND: 36.5g +/- 3.1). Orange dotted lines represent traces from control ND mice in Fig. 1. Orange squares are measures in age-matched control mice at 52 weeks. C. Reversal of visual decline was evident after 6 weeks of drug treatment, (MTP-131: 0.211 c/d +/- 0.003 vs 0.198 c/d +/- 0.003, $p<0.05$) and recovery to 80% normal (MTP-131: 0.311 c/d +/- 0.003 vs Veh: 0.152 c/d +/- 0.003 vs ND: 0.393 c/d +/- 0.001) was evident by 52 weeks. Dotted orange line depicts the function of ND mice, and teal line is the effect of MTP-131 eye drop treatment, from Fig. 5C.

Translational Impact:

(1) Clinical issue: Current treatments for visual dysfunction in diabetes are focused on managing the symptoms of diabetes, such as hyperglycemia, obesity and retinal edema in the non-proliferative phase, and on improving clarity of the optical axis, or controlling retinal angiogenesis and its consequences in the proliferative stage. These treatments have limited efficacy, and able to slow, but not reverse, visual decline. Our work describes a novel approach to treating diabetic visual dysfunction based on targeting and treating mitochondrial dysfunction with a water-soluble peptide (MTP-131).

(2) Results: We find that progressive decline of spatial visuomotor function emerges in mouse models of Type 1 and Type 2 diabetes early in the course of disease; before typical symptoms of diabetes, such as hyperglycemia and obesity, are present. Both systemic and eye-drop application of MTP-131 early in the course of visual decline, are able to prevent further decline and fully reverse dysfunction without normalizing aberrant glucose clearance,

or elevated blood glucose and weight. Equivalent treatment later in disease, after much more severe visual dysfunction is manifest, is also able to substantially restore function.

(3) Implications and future directions: These data indicate that mitochondrial dysfunction, which may be detected with spatial measures of visuomotor function, is an early and treatable pathophysiology of diabetes that is independent of the other symptoms of metabolic dysfunction. They also indicate that improving mitochondrial function can treat the visual dysfunction without remediating glucose dysregulation or obesity. Thus, mitochondrial-based treatment on its own, or in combination with current therapies, may provide a new and more effective approach to treating the visual consequences of diabetes at any stage of disease. Since MTP-131 has an exceptional human safety profile it has the potential to be rapidly translated into clinical trials.

Figure 1

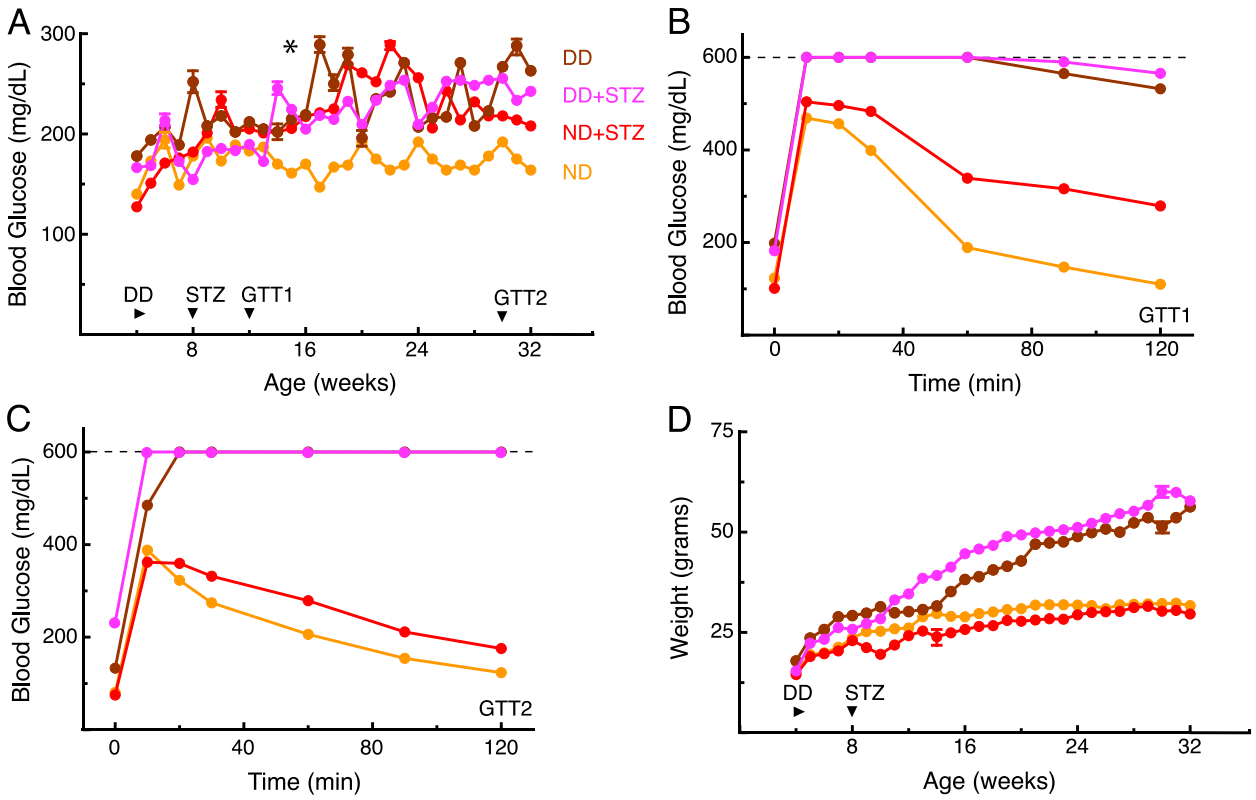

Figure 2

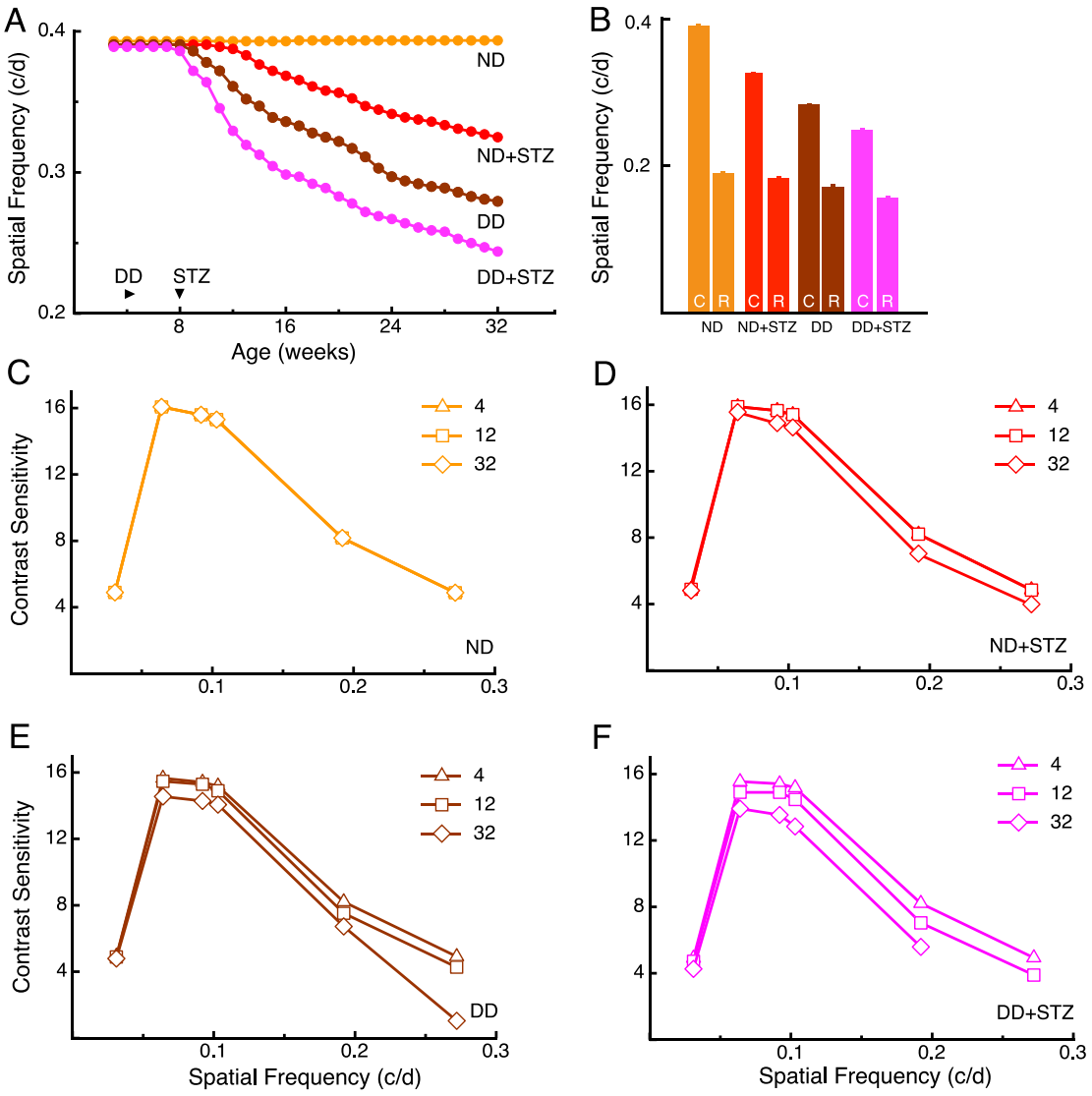

Figure 3

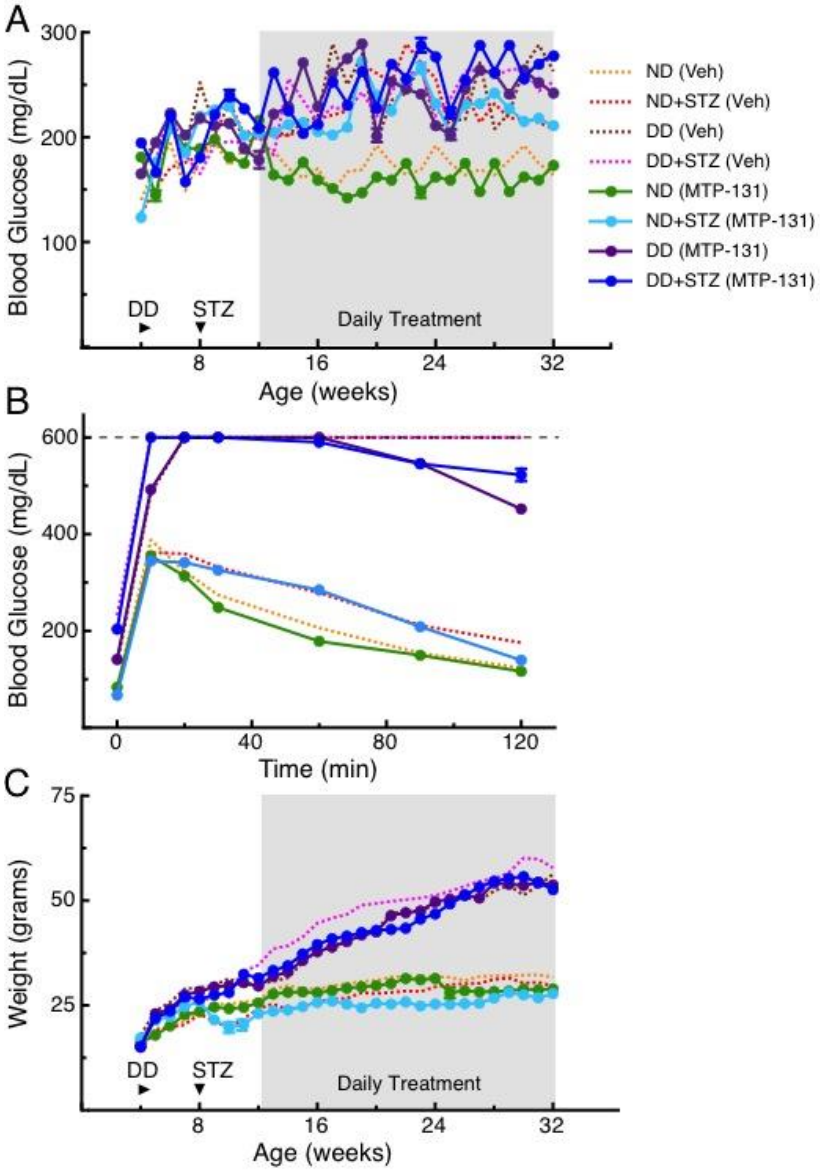

Figure 4

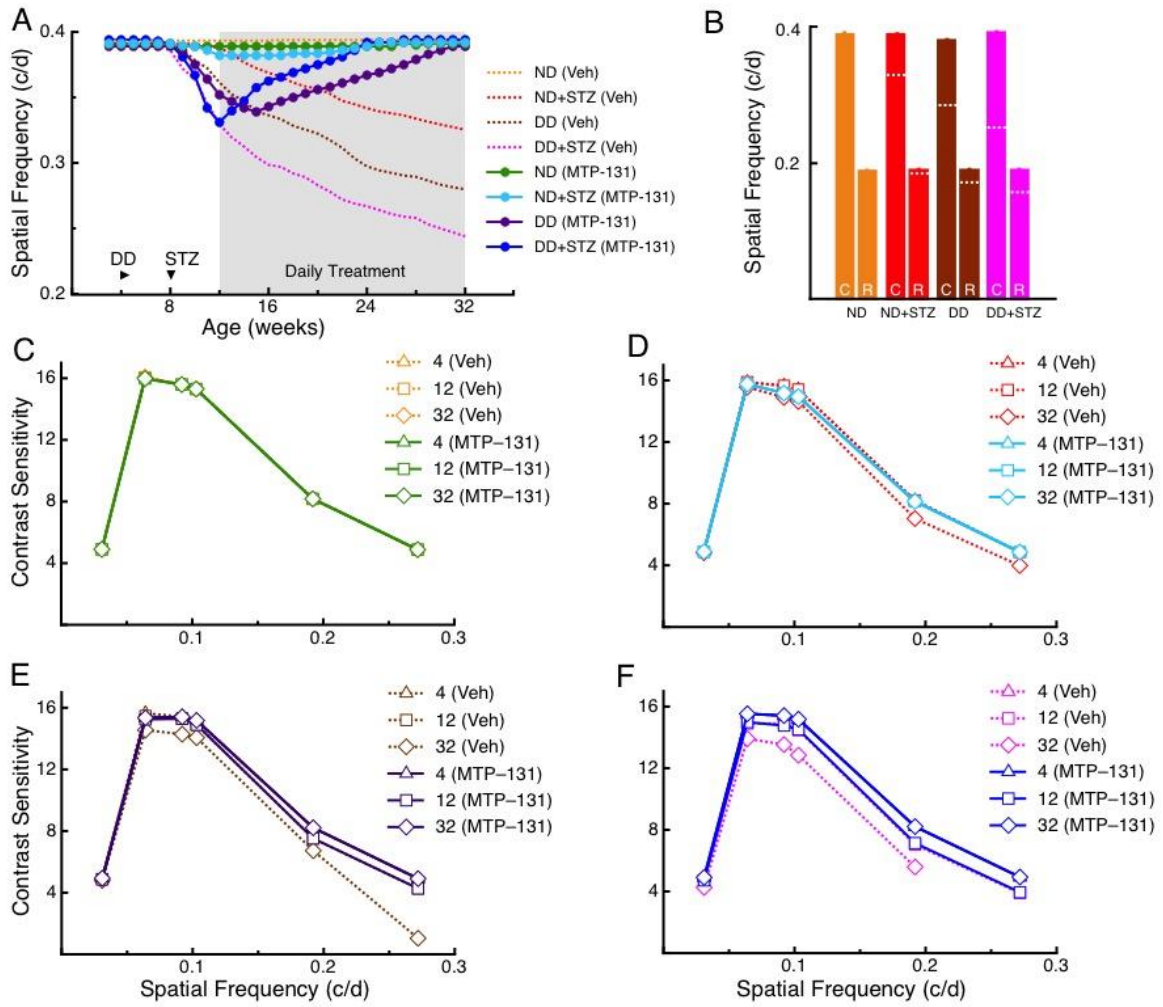

Figure 5

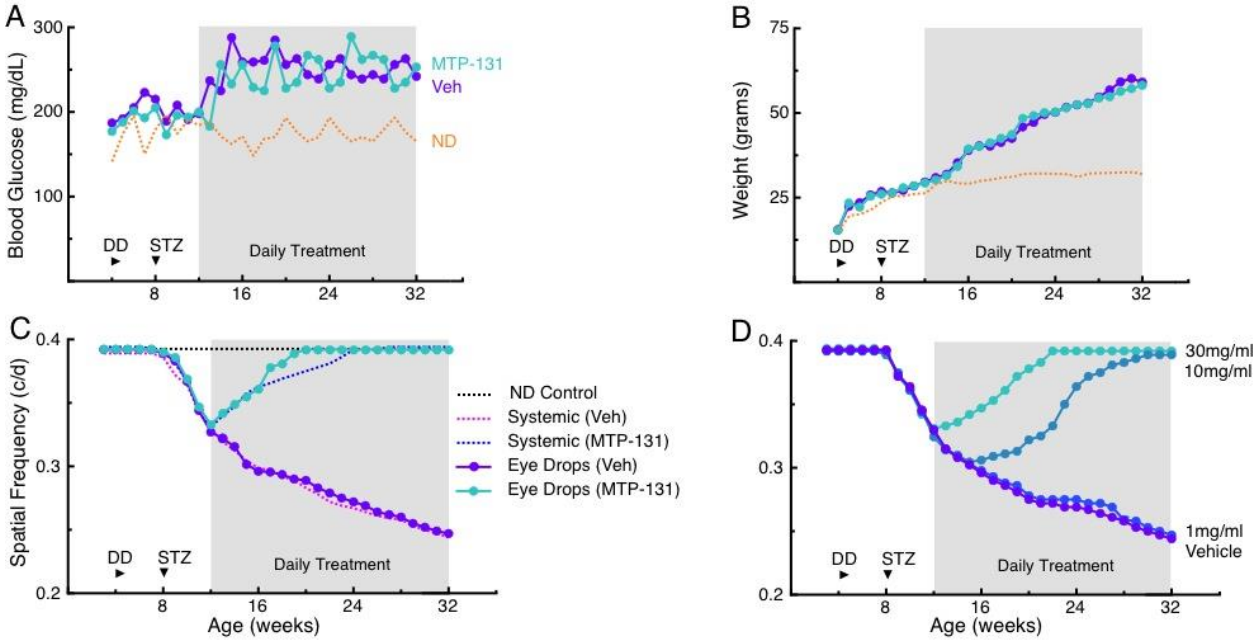

Figure 6